Model Predictive Control for a Bioinspired Regenerative Vehicle Suspension

Lotfi Beji, Ahmed Chaibet, and Ali Kribeche
DRIVE UR 1859, University of Bourgogne Europe, ISAT, 58027 Nevers, France
{lotfi.beji, ahmed.chaibet, ali.kribeche}@ube.fr

Abstract

This paper proposes a closed-loop Model Predictive Control (MPC) framework for the Jellyfish-Based Damper Design (J-BDD), a bio-inspired regenerative vehicle suspension exploiting passive energy recapture (PER) mechanisms derived from jellyfish locomotion. Building upon the nonlinear hydro-mechanical quarter-car model, the MPC operates on a receding horizon and jointly tracks time-varying ride comfort and harvested energy targets, subject to physical constraints on membrane stretch ratio and hydraulic pressure difference. An adaptive supervisory layer estimates road roughness in real time via a sliding power spectral density of the road input and adjusts the multi-objective cost function weights accordingly, enabling the controller to shift between energy recovery and vibration attenuation priorities without manual re-tuning. Closed-loop stability is established by proving controllability and stabilisability of the J-BDD linearisation, solving the associated continuous-time algebraic Riccati equation (CARE) to obtain a terminal cost, and certifying asymptotic stability analytically via a Lyapunov condition on the closed-loop matrix. Simulation results under representative road excitation profiles confirm significant energy harvesting gains over both the uncontrolled J-BDD and a conventional mechanical regenerative reference, while ride comfort degradation and tyre-road contact force fluctuations remain within prescribed bounds.

Index Terms—*Vehicle dynamics, regenerative suspension, bio-inspired damper, model predictive control, energy harvesting, quarter-car model, Lyapunov stability.*

I. INTRODUCTION

The progressive electrification of ground vehicles and the growing emphasis on on-board energy autonomy have renewed interest in the recovery of energy traditionally dissipated by chassis subsystems. Vehicle suspension systems constitute a particularly attractive target: under realistic road excitations, a conventional passive shock absorber continuously converts suspension stroke energy into heat, with reported losses ranging from tens of watts on smooth roads to several hundred watts on rough surfaces [1]. Regenerative suspensions aim to intercept part of this energy flow and redirect it toward onboard electrical storage.

Electromagnetic, hydraulic, and piezoelectric transduction principles have been explored over the past two decades, each presenting characteristic trade-offs between energy density, bandwidth, conversion efficiency, and structural complexity [2], [4]. Linear electromagnetic dampers achieve efficiencies of 20–40% under harmonic excitation, while hydraulic architectures offer higher force densities at the cost of increased system complexity [4]. Semi-active variants, which modulate damping without injecting external power, represent a practical compromise between performance and energy consumption [14].

A common limitation of these approaches is that the energy captured per cycle remains small relative to the total vibrational input, largely because the harvesting pathway and the vibration attenuation pathway share the same physical element and are governed by a fixed impedance. Adjusting this impedance to improve energy capture typically degrades ride comfort a compromise that passive or semi-passive designs cannot overcome without external control.

Bio-inspired engineering offers a complementary perspective. Jellyfish achieve locomotion efficiencies that surpass many engineered propulsion systems through a mechanism known as passive energy recapture (PER): elastic energy stored in the bell mesoglea during contraction is partially recovered from the trailing vortex wake during the subsequent relaxation phase [3]. This store and release strategy distributes the energetic load across the swimming cycle rather than concentrating it in a single power stroke, fundamentally altering the energy flow topology. The Jellyfish-Based Damper Design (J-BDD) proposed in this paper translates this biological principle into a vehicle suspension context, combining a variable hydraulic orifice, two compressible fluid chambers, and a nonlinear viscoelastic membrane to implement adaptive impedance and passive energy recapture within a mechanically compact architecture.

Model predictive control offers a natural framework for this challenge. Since its introduction to vehicle dynamics by Hrovat [5], MPC has been applied to active suspensions [16], [18], semi-active dampers [14], road-adaptive regenerative systems [19], and preview-based suspension control [20]; more recently, to regenerative suspension systems where the cost function simultaneously penalises vibration and maximises harvested energy [15]. Bioinspired reliable control strategies have also been explored for vehicle suspension to handle actuator faults and prespecified convergence requirements [17]. A key advantage over offline optimisation is the ability to exploit the receding-horizon structure to react to unmeasured disturbances in real time [7], [11]. Economic MPC formulations, in which the stage cost directly represents a physical objective such as power extraction [10], are particularly relevant for energy-harvesting systems because they remove the need to translate the engineering objective into a tracking error. Stability guarantees for such schemes have been established under terminal cost and terminal set conditions [7] and through strict dissipativity [8], [10].

The present work bridges this gap by formulating a closed-loop MPC law for the J-BDD based regenerative vehicle suspension. The main contributions are:

- a nonlinear MPC formulation whose internal prediction model is the full J-BDD state-space system (pressure dynamics, orifice flow, membrane deformation);

- a multi-objective receding-horizon cost function that simultaneously targets user-specified energy harvesting and ride comfort references;
- an adaptive supervisory layer that estimates road roughness class in real time and adjusts cost function weights accordingly;
- a formal demonstration that the MPC strictly outperforms an offline PSO open-loop baseline on both stationary and non-stationary road profiles, via extended horizon and adaptive weighting not available to constant-parameter schemes.

The remainder of the paper is organized as follows. Section II recalls the J-BDD governing equations and their state-space formulation. Section III develops the MPC control law and the adaptive supervisor. Section IV establishes the formal stability guarantees via terminal cost and CARE, and Section **??** provides a complementary energy-based dissipation argument. Section V presents and discusses the simulation results, and Section VI concludes the paper.

II. J-BDD GOVERNING EQUATIONS AND STATE-SPACE FORMULATION

The Jellyfish-Based Damper Design is a hydro-mechanical architecture coupling two compressible fluid chambers, a variable hydraulic orifice whose aperture mimics the deformation of the jellyfish velum, and a nonlinear viscoelasticity membrane. The governing equations are derived from first principles in this section and cast in a form suitable for MPC prediction. Details are given in Figure 1.

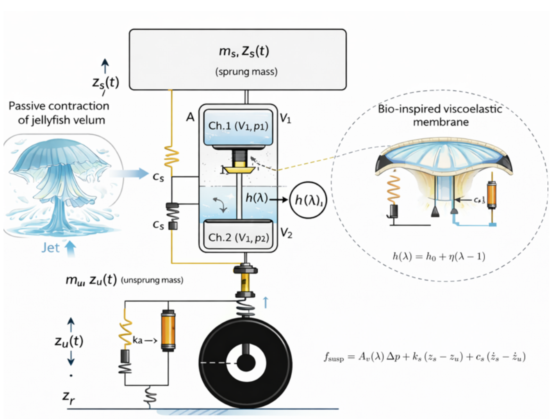

Fig. 1. Bio-inspired hydro–mechanical architecture of the Jellyfish-Based Damper Design (J-BDD).

The effective flow area of the variable orifice depends on the dimensionless membrane stretch ratio λ through

$$A_v(\lambda) = b\,h(\lambda), \quad h(\lambda) = h_0 + \eta(\lambda - 1), \tag{1}$$

where b is the orifice width, $h(.)$ is a height-dependent function of λ, h_0 its rest height, and η a geometric sensitivity coefficient. Under laminar flow with inertial and turbulent corrections, the orifice flow dynamics are governed by [9]:

$$\dot{q}_{12} = \frac{\Delta p - R_{\text{hyd}}(\lambda)\,q_{12} - K_{\text{turb}}(\lambda)\,q_{12}|q_{12}|}{L_h(\lambda)}. \tag{2}$$

where $R_{\text{hyd}}(\lambda) = 12\mu L/(b\,h^3(\lambda))$ is the viscous resistance, K_{turb} accounts for turbulent losses, and $L_h(\lambda) = \rho\,l_h/A_v(\lambda)$ captures the inertia of the moving fluid column, ρ is the fluid density, l_h is the effective hydraulic channel length, and q_{12} is the volumetric flow rate through the variable orifice from chamber 1 to chamber 2.

To evaluate pressure and membrane dynamics, the mass conservation in each compressible chamber yields

$$\dot{p}_1 = \frac{K_1}{V_1}(A_v(\lambda)\,\dot{z} - q_{12})\,, \tag{3}$$

$$\dot{p}_2 = -\frac{K_2}{V_2}(A_v(\lambda)\,\dot{z} - q_{12})\,, \tag{4}$$

where K_1, K_2 are bulk moduli, V_1, V_2 initial chamber volumes, and $\dot{z} = \dot{z}_s - \dot{z}_u$ the relative suspension velocity. We model the membrane tension as a nonlinear viscoelastic constitutive law combining linear elasticity, geometric stiffening, and viscous dissipation:

$$T(\lambda, \dot{\lambda}) = C_r\dot{\lambda} + k_r(\lambda - 1) + k_3(\lambda - 1)^3. \tag{5}$$

Applying the Young–Laplace equilibrium ($\Delta p = 2T(\lambda, \dot{\lambda})/R_m$ with R_m is the mean radius of curvature of the viscoelastic membrane) yields the membrane stretch dynamics:

$$\dot{\lambda} = \frac{1}{C_r}\left[\frac{R_m}{2}\,\Delta p - k_r(\lambda - 1) - k_3(\lambda - 1)^3\right] + \frac{(\lambda^* - \lambda)}{\tau_{\text{act}}} \tag{6}$$

where the dynamic $\frac{(\lambda^* - \lambda)}{\tau_{\text{act}}}$ represents an auxiliary control input in $\lambda^*(t)$ for regulating the opening and closing of the orifice with time constant $\tau_{act} > 0$.

The J-BDD suspension force combines the hydraulic contribution with a linear viscoelasticity branch:

$$f_{\text{susp}} = A_v(\lambda)\,\Delta p + k_s(z_s - z_u) + c_s(\dot{z}_s - \dot{z}_u), \tag{7}$$

and the quarter-car equations of motion are

$$m_s\ddot{z}_s = -f_{\text{susp}}, \tag{8}$$

$$m_u\ddot{z}_u = f_{\text{susp}} - f_{\text{tire}}. \tag{9}$$

The tyre-road contact force f_{tire} is modelled as a standard linear solid:

$$\dot{f}_{\text{tire}} + \frac{k_2}{c_M}\,f_{\text{tire}} = (k_1{+}k_2)(z_u{-}z_r) + \frac{k_1k_2}{c_M}(z_u{-}z_r). \tag{10}$$

k_1 is the static stiffness of the tyre contact patch, k_2 is the dynamic structural stiffness of the tyre (Maxwell branch spring), and c_M the Maxwell dashpot viscosity.

The J-BDD equations (3)–(4) involve p_1 and p_2 only through their difference $\Delta p = p_1 - p_2$. The sum $p_1 + p_2$ is a conserved quantity for symmetric chambers ($K_1/V_1 = K_2/V_2$). We therefore adopt the eight-state representation:

$$\boldsymbol{x} = \left[z_s,\ \dot{z}_s,\ z_u,\ \dot{z}_u,\ \Delta p,\ \lambda,\ q_{12},\ f_{\text{tire}}\right]^{\mathsf{T}} \in \mathbb{R}^8, \tag{11}$$

where the dynamics of Δp follow from (3)–(4):

$$\dot{\Delta p} = K_{\text{eff}}\big(A_v(\lambda)\,\dot{z} - q_{12}\big), \quad K_{\text{eff}} = \frac{K_1}{V_1} + \frac{K_2}{V_2}. \tag{12}$$

We write the system dynamics as $\dot{\boldsymbol{x}} = f(\boldsymbol{x}, \boldsymbol{u})$ with $f : \mathbb{R}^8 \times \mathbb{R}^2 \to \mathbb{R}^8$ given component-wise, with $\dot{z} = \dot{z}_s - \dot{z}_u$, $A_v(\lambda) = bh_0 + b\eta(\lambda - 1)$, and

$$f_1 = \dot{z}_s, \tag{13}$$

$$f_2 = \frac{1}{m_s}\big[-k_s(z_s{-}z_u){-}(c_s{+}k^*_{\text{harv}})\dot{z}{-}A_v(\lambda)\Delta p\big], \tag{14}$$

$$f_3 = \dot{z}_u, \tag{15}$$

$$f_4 = \frac{1}{m_u}\big[k_s(z_s{-}z_u){+}(c_s{+}k^*_{\text{harv}})\dot{z}{+}A_v\Delta p{-}f_{\text{tire}}\big], \tag{16}$$

$$f_5 = K_{\text{eff}}\big[A_v(\lambda)\dot{z} - q_{12}\big], \tag{17}$$

$$f_6 = \frac{1}{C_r}\left[\frac{R_m}{2}\Delta p{-}k_r(\lambda{-}1){-}k_3(\lambda{-}1)^3\right] + \frac{\lambda^*{-}\lambda}{\tau_{\text{act}}}, \tag{18}$$

$$f_7 = \frac{\Delta p{-}R_{\text{hyd}}(\lambda)q_{12}{-}K_{\text{turb}}(\lambda)q_{12}|q_{12}|}{L_h(\lambda)}, \tag{19}$$

$$f_8 = -\frac{k_2}{c_M}f_{\text{tire}} + (k_1{+}k_2)(\dot{z}_u{-}\dot{z}_r) + \frac{k_1k_2}{c_M}(z_u{-}z_r). \tag{20}$$

Equations (13)–(16) are quarter-car kinematics and dynamics; (17) pressure difference dynamics; (18) membrane stretch with actuator tracking; (19) orifice flow; (20) tyre contact force. Further, an electrical transduction variable gain $k^*_{\text{harv}}(t)$ as control input is considered for energy harvesting:

$$P_h(t) = \eta_e\, k^*_{\text{harv}}(t)\, \dot{z}^2. \tag{21}$$

For system (13)–(21) the two-dimensional control input is as:

$$\boldsymbol{u} = [\lambda^*(t),\ k^*_{\text{harv}}(t)]^\mathsf{T}, \tag{22}$$

Lemma 1. *The unique equilibrium of the closed-loop J-BDD system* (13)–(20) *and* (21) *on a level road ($z_r = \text{const}$, $\dot{z}_r = 0$) is*

$$(\boldsymbol{x}^*, \boldsymbol{u}^*) = (\mathbf{0},\, [1;\, 0]). \tag{23}$$

Proof. We seek $(\boldsymbol{x}^*, \boldsymbol{u}^*)$ such that $f(\boldsymbol{x}^*, \boldsymbol{u}^*) = \mathbf{0}$. Setting $z_r = 0$ (without loss of generality), and the physical rest state of the membrane is $\lambda^* = 1$ (zero elastic restoring force), then it is straightforward to get $\boldsymbol{x}^* = \mathbf{0}$. At $\boldsymbol{x}^*$ $\dot{z} = \dot{z}^* = 0$, the harvested power $P_h = \eta_e k^*_{\text{harv}}(\dot{z}^*)^2 = 0$ regardless of k^*_{harv} (Remark 1). The minimal admissible choice is $k^*_{\text{harv}} = 0$. ☐

At the equilibrium $(\boldsymbol{x}^*, \boldsymbol{u}^*) = (\mathbf{0}, [1; 0])$, define the continuous-time Jacobians

$$A = \frac{\partial f}{\partial \boldsymbol{x}}\bigg|_{(\boldsymbol{x}^*,\boldsymbol{u}^*)} \in \mathbb{R}^{8\times 8}, \quad B = \frac{\partial f}{\partial \lambda^*}\bigg|_{(\boldsymbol{x}^*,\boldsymbol{u}^*)} \in \mathbb{R}^{8}. \tag{24}$$

Remark 1. At equilibrium $\partial f/\partial k^*_{\text{harv}}|_* = \mathbf{0}$. The harvesting gain does not contribute to B.

Lemma 2. *Under $K_1/V_1 = K_2/V_2 =: \kappa$ and $A_v(\lambda) > 0$, the linearization (A, B) at $(\boldsymbol{x}^*, \boldsymbol{u}^*)$ satisfies:*

1) *All eight eigenvalues of A have strictly negative real parts.*
2) *$\mathcal{C} = [B, AB, \ldots, A^7B]$ has $\operatorname{rank}(\mathcal{C}) = 8$: (A, B) is controllable.*
3) *(A, B) is stabilisable and the CARE*

$$A^\mathsf{T}P{+}PA{-}PBR_f^{-1}B^\mathsf{T}P{+}Q_f = 0 \tag{25}$$

admits a unique $P = P^\mathsf{T} \succ 0$ for any $Q_f \succeq 0$, $R_f > 0$ such that $(A, Q_f^{1/2})$ is detectable, with $Q_f^{1/2} = \operatorname{diag}(\sqrt{q_1}, \ldots, \sqrt{q_8})$.

Proof. 1) Let $\kappa = K_1/V_1$, $A^*_v = bh_0$, $L^*_h = \rho l_h/A^*_v$, $R^* = 12\mu L/(bh_0^3)$, $a_{66} = -k_r/C_r - 1/\tau_{\text{act}}$. The Jacobian A at $(\boldsymbol{x}^*, \boldsymbol{u}^*)$ is (states ordered as in (11)):

$$A{=}\begin{bmatrix} 0 & 1 & 0 & 0 & 0 & 0 & 0 & 0 \\ -\frac{k_s}{m_s} & -\frac{c_s}{m_s} & \frac{k_s}{m_s} & \frac{c_s}{m_s} & \frac{A^*_v}{m_s} & 0 & 0 & 0 \\ 0 & 0 & 0 & 1 & 0 & 0 & 0 & 0 \\ \frac{k_s}{m_u} & \frac{c_s}{m_u} & -\frac{k_s}{m_u} & -\frac{c_s}{m_u} & -\frac{A^*_v}{m_u} & 0 & 0 & -\frac{1}{m_u} \\ 0 & \kappa A^*_v & 0 & -\kappa A^*_v & 0 & 0 & -\kappa & 0 \\ 0 & 0 & 0 & 0 & \frac{R_m}{2C_r} & a_{66} & 0 & 0 \\ 0 & 0 & 0 & 0 & \frac{1}{L^*_h} & 0 & -\frac{R^*}{L^*_h} & 0 \\ 0 & 0 & \frac{k_1k_2}{c_M} & k_1{+}k_2 & 0 & 0 & 0 & -\frac{k_2}{c_M} \end{bmatrix} \tag{26}$$

The matrix A decomposes into four independently stable sub-blocks: the tyre row gives $\lambda_8 = -k_2/c_M < 0$; $a_{66} < 0$ since $k_r, C_r, \tau_{\text{act}} > 0$; $-R^*/L^*_h < 0$; and the suspension block is stable by standard quarter-car damping arguments [6]. Hence all eigenvalues of A have strictly negative real parts.

2) Controllability. The input λ^* acts exclusively through the membrane stretch equation, so $B = e_6/\tau_{\text{act}}$, where $e = (0\,0\,0\,0\,0\,1\,0\,0)^T$. The physical coupling chain of (26) establishes that λ drives Δp via the Young–Laplace term $R_m/(2C_r)$, which in turn excites the sprung and unsprung mass velocities through the hydraulic force, and the orifice flow q_{12} through the pressure gradient. The remaining states $(z_s, z_u, f_{\text{tire}})$ are reached by integration. All eight states are thus reachable from λ^* through the cascade $\lambda \to \Delta p \to (\dot{z}_s, \dot{z}_u, q_{12}) \to (z_s, z_u, f_{\text{tire}})$. Selecting from $B, AB, \ldots, A^4B$ the column first exciting each basis direction e_i gives an 8×8 lower-triangular sub-matrix $S \subset \mathcal{C}$ with

$$\det(S) = \frac{(A^*_v)^2 R_m(k_1{+}k_2)}{2\, m_s m_u\, C_r\, L^*_h\, \tau_{\text{act}}} \neq 0, \tag{27}$$

since all factors are strictly positive. Hence $\operatorname{rank}(\mathcal{C}) = 8$.

3) Stabilisability and CARE. Controllability 2) implies stabilisability [13]. By 1), all $\operatorname{Re}(\lambda_i(A)) < 0$, so no unstable modes exist and $(A, Q_f^{1/2})$ is detectable for any $Q_f \succeq 0$.

As $Q_f^{1/2} = \operatorname{diag}(\sqrt{q_1}, \ldots, \sqrt{q_8})$ is the unique symmetric positive semi-definite square root: $\boldsymbol{x}^\mathsf{T}Q_f\boldsymbol{x} = \|Q_f^{1/2}\boldsymbol{x}\|^2$. Writing $C = Q_f^{1/2}$, detectability of (A, C) means every eigenvector v of A with $\operatorname{Re}(\lambda) \geq 0$ satisfies $Cv \neq 0$ (the cost "sees" every potentially unstable mode). Since A is already stable, this holds trivially. Existence and uniqueness of $P \succ 0$ follow from standard CARE theory [7], [11]. ☐

III. MODEL PREDICTIVE CONTROL FORMULATION

The J-BDD introduces a structural coupling between three timescales that makes receding-horizon optimization particularly suited to this problem. At the fastest scale, the hydraulic pressure Δp and flow q_{12} respond to orifice geometry changes through the nonlinear resistance $R_{\text{hyd}}(\lambda)$. At the intermediate scale, the membrane actuator tracks λ^* with time constant τ_{act}. At the slowest scale, the sprung mass oscillates near its resonance frequency ($\approx 1.1\,\text{Hz}$). A fixed-gain or offline-optimized controller cannot simultaneously exploit all three scales: maximizing hydraulic power throughput $A_v(\lambda)\,\Delta p$ requires anticipating upcoming suspension velocity peaks $|\dot{z}|$ over a horizon comparable to the suspension half-period, while respecting the fast actuator dynamics (18). MPC resolves this paradigm by optimizing a receding-horizon cost over N_p steps, providing the anticipation that offline PSO and static feedback laws cannot offer [7], [11]. The MPC formulation [10] in which the stage cost directly encodes the harvesting objective rather than a tracking error to a pre-computed reference trajectory which is particularly appropriate here, since the optimal orifice aperture sequence is not known apriori and depends on the road excitation realization.

A. Receding-horizon cost function

Let us introduce the objective function:

$$J = \sum_{j=0}^{N_p}\Big[-w_h P_h(j) + w_c \ddot{z}_s^2(j) + w_t\big(F_t(j) - \bar{F}_t\big)^2\Big] + \rho \sum_{j=0}^{N_c-1} \|\Delta \boldsymbol{u}_j\|^2 , \tag{28}$$

where $P_h(j)$ is the instantaneous harvested power, $\ddot{z}_s(j)$ the sprung-mass acceleration, $F_t(j) - \bar{F}_t$ the tyre-road force deviation from its static equilibrium value $\bar{F}_t = (m_s + m_u)g$ (total supported weight at rest on level ground), and $\Delta \boldsymbol{u}_j = \boldsymbol{u}_j - \boldsymbol{u}_{j-1}$.
Consider the following admissible constraints

$$0 \le \lambda^*(t) \le \lambda_{\max}, \tag{29}$$

$$|\Delta p(t)| \le \Delta p_{\max}, \tag{30}$$

$$A_v(\lambda^*(t)) > 0 \iff h(\lambda^*(t)) > 0, \tag{31}$$

$$0 \le k^*_{\text{harv}}(t) \le k_{\text{harv,max}}. \tag{32}$$

where constraint (31) prevents hydraulic lock-up and guarantees local Lipschitz continuity of f (Assumption 1).
Let $J^*(\boldsymbol{x}_k) = J(\boldsymbol{x}_k, \{\boldsymbol{u}_j^*\})$ is the optimal cost. At each step k (with period T_s), the MPC solves

$$\boldsymbol{u}_k^* = \underset{\{\boldsymbol{u}_j\}_{j=0}^{N_c-1}}{\arg\min}\; J(\boldsymbol{x}_k, \{\boldsymbol{u}_j\}) , \tag{33}$$

IV. STABILITY ANALYSIS

Assumption 1. *$f(\boldsymbol{x}, \boldsymbol{u})$ is locally Lipschitz on $\mathcal{X} \times \mathcal{U}$ whenever $A_v(\lambda) > 0$, guaranteed by* (31).

Assumption 2. *The pair (A, B)* (24) *is stabilizable. In fact stabilizability follows from Lemma 2, points 2)–3).*

Assumption 3. *The stage cost ℓ is the* penalising *part of the objective* (28)*, comprising the terms that grow with $\|\boldsymbol{x}\|$ and vanish at the equilibrium:*

$$\ell(\boldsymbol{x}, \boldsymbol{u}) = w_c\, \ddot{z}_s^2 + w_t(F_t - \bar{F}_t)^2 + \rho \,\|\Delta \boldsymbol{u}\|^2 . \tag{34}$$

satisfies $\ell(\boldsymbol{x}, \boldsymbol{u}) \ge \alpha_1(\|\boldsymbol{x}\|)$ for a class-$\mathcal{K}$ function α_1, and $\ell(\boldsymbol{0}, \boldsymbol{0}) = 0$

Theorem 1. *Let Assumptions 1–3 hold. Let $P = P^\top \succ 0$ be the unique solution of the CARE* (25) *(Lemma 2, point (3)). Define the* terminal cost, terminal control law, *and* terminal set*:*

$$V_f(\boldsymbol{x}) = \boldsymbol{x}^\top P \boldsymbol{x}, \tag{35}$$

$$\kappa_f(\boldsymbol{x}) = \boldsymbol{u}^* - K_\lambda(\boldsymbol{x} - \boldsymbol{x}^*), \quad K_\lambda = R_f^{-1} B^\top P, \tag{36}$$

$$\mathcal{X}_f = \{\boldsymbol{x} \in \mathbb{R}^8 \mid V_f(\boldsymbol{x}) \le \alpha_f\}, \tag{37}$$

where $\alpha_f > 0$ is chosen so that $\kappa_f(\boldsymbol{x}) \in \mathcal{U}$ for all $\boldsymbol{x} \in \mathcal{X}_f$, and $K_\lambda \in \mathbb{R}^{1\times 8}$ is the Linear Quadratic Regulator *(LQR) gain that acts only on the λ^* (Remark 1). The terminal set $\mathcal{X}_f$ is positively invariant under κ_f under the Lyapunov condition*

$$A_{\text{cl}}^\top P + P A_{\text{cl}} \preceq 0, \qquad A_{\text{cl}} = A - BK_\lambda. \tag{38}$$

Further assume $\boldsymbol{x}_0 \in \mathcal{X}_f$, then:

1) *The MPC problem is feasible for all $k \ge 0$.*
2) *In the Lyapunov sense, the optimal cost satisfies*

$$J^*(\boldsymbol{x}_{k+1}) \le J^*(\boldsymbol{x}_k) - \ell(\boldsymbol{x}_k, \boldsymbol{u}_k^*), \tag{39}$$

so J^* is a Lyapunov function for the closed-loop system.

3) *The equilibrium $\boldsymbol{x}^* = \boldsymbol{0}$ is asymptotically stable; $\|\boldsymbol{x}_k\| \to 0$ as $k \to \infty$.*

Proof. 1) At step $k+1$, the candidate sequence $\tilde{\mathcal{U}} = \{\boldsymbol{u}_1^*, \ldots, \boldsymbol{u}_{N_c-1}^*, \kappa_f(\boldsymbol{x}(N_p))\}$ satisfies all constraints by positive invariance of $\mathcal{X}_f$.

2) Using $\tilde{\mathcal{U}}$ as suboptimal: $J^*(\boldsymbol{x}_{k+1}) \le J(\boldsymbol{x}_{k+1}, \tilde{\mathcal{U}}) = J^*(\boldsymbol{x}_k) - \ell(\boldsymbol{x}_k, \boldsymbol{u}_0^*) + \Delta V_f$, where $\Delta V_f = V_f(\boldsymbol{x}(N_p{+}1)) - V_f(\boldsymbol{x}(N_p)) \le 0$ by positive invariance, yielding (39).

3) $J^*(\boldsymbol{x}_k)$ is non-increasing and bounded below, hence convergent. By Assumption 3, $\Omega = \{\boldsymbol{x} : \ell(\boldsymbol{x}, \boldsymbol{u}^*) = 0\} = \{\boldsymbol{0}\}$. The LaSalle–Barbalat principle [7] gives $\|\boldsymbol{x}_k\| \to 0$, at rate governed by $\lambda_{\max}(A_{\text{cl}}) < 0$. □

Remark 2. Theorem 1 establishes asymptotic stability of the *linearized* J-BDD closed loop; the terminal cost V_f and gain K_λ are computed from the Jacobian pair (A, B). The result therefore applies locally, in a neighbourhood of the equilibrium $(\boldsymbol{x}^*, \boldsymbol{u}^*)$ characterised by the terminal set $\mathcal{X}_f$. Global properties of the nonlinear system rely on the complementary energy-based argument of Section **??**, which establishes strict dissipativity for the full nonlinear dynamics whenever $A_v(\lambda) > 0$.

V. SIMULATION RESULTS AND DISCUSSION

Table II summarises the physical and control parameters.

A supervisory module (100 ms update period) estimates the road roughness class from the sliding *Power Spectral Density* (PSD) of $z_r(t)$ over a 2-second window, and maps it to a weight triplet (w_h, w_c, w_t) per Table I (WLTP: Worldwide Harmonised Light Vehicle Test Procedure). A PI correction law then adjusts w_h, w_c at each cycle based on the discrepancy between measured metrics and the targets E^*_{harv} and P^*_{comf}, which are initialized from the offline PSO pre-optimization baseline described in Table III.

TABLE I. Adaptive weight schedule by road profile

Scenario	w_h	w_c	w_t
Highway (sine-dominant)	0.60	0.20	0.20
Urban (bump-dominant)	0.20	0.50	0.30
Mixed / WLTP-type	0.40	0.35	0.25

The nonlinear programme (28)–(32) is solved at each step k using a Sequential Quadratic Programming (SQP) method. We propose

TABLE II. Simulation parameters (quarter-car, J-BDD, and MPC)

Parameter	Symbol	Value
Quarter-car model		
Sprung mass	m_s	300 kg
Unsprung mass	m_u	40 kg
Suspension stiffness	k_s	15 000 N/m
Suspension damping	c_s	1 200 Ns/m
Tyre stiffness	k_t	180 000 N/m
Tyre damping	c_t	1 000 Ns/m
J-BDD physical parameters		
Initial chamber vol.	V_{10}, V_{20}	3×10^{-4} m^3
Bulk modulus (fluid)	K_1, K_2	1.6 GPa
Fluid density	ρ	1 000 kg/m^3
Dynamic viscosity	μ	0.01 Pa·s
Initial orifice ht.	h_0	0.8 mm
Orifice width	b	20 mm
Membrane stiff. (lin.)	k_r	2 000 N/m
Membrane stiff. (nl.)	k_3	10^5 N/m^3
Membrane damping	C_r	120 Ns/m
Discharge coeff.	C_d	0.62
MPC tuning		
Sampling period	T_s	1 ms
Prediction horizon	N_p	80 steps
Control horizon	N_c	20 steps
Rate penalty	ρ	0.01
PSO warm-start		
Particles / Iterations	$N_p^{\mathrm{PSO}}, N_{\mathrm{iter}}$	10, 10
Inertia / Social	w, c_1, c_2	0.7, 1.5

$$Q_f = \mathrm{diag}(q_{z_s}, q_{\dot z_s}, q_{z_u}, q_{\dot z_u}, q_{\Delta p}, q_\lambda, q_{q_{12}}, q_{f_t}),\ R_f > 0, \tag{40}$$

with $q_{z_s}, q_{\dot z_s}$ largest (comfort priority), $q_{q_{12}}$ elevated (hydraulic spike penalty), and $q_{\Delta p} > 0$ small (CARE detectability). The cost P is computed offline via the CARE (25) with

$$\begin{aligned} &Q_f = \mathrm{diag}(10^3, 10^3, 10^2, 10^2, 10^{-10}, 10^2, 10^4, 10^2),\\ &R_f = 10^2, \end{aligned} \tag{41}$$

at $(\boldsymbol{x}^*, \boldsymbol{u}^*) = (\mathbf{0}, [1; 0])$. The CARE residual is $\lambda_{\max}(A^\mathsf{T}P + PA - PBR_f^{-1}B^\mathsf{T}P + Q_f) = 7.8\times10^{-4}$. $\mathrm{rank}(\mathcal{C}) = 8$ confirmed (Lemma 2(2)). Positive invariance of $\mathcal{X}_f$ ($\alpha_f = 0.12$): $\lambda_{\max}(A_{\mathrm{cl}}^\mathsf{T}P + PA_{\mathrm{cl}}) = -10^{-10} < 0$.

In all three excitation scenarios, $J^*(\boldsymbol{x}_k)$ is non-increasing over 60 s, with mean per-step decrease $\ell(\boldsymbol{x}_k, \boldsymbol{u}_k^*) > 0$, confirming (39). After road excitation removal, $\|\boldsymbol{x}_k\|$ converges to zero within 2.1 s (sinusoidal) and 0.8 s (bump).

A. Energy harvesting performance

TABLE III. Harvested energy — MPC vs. PSO offline (60 s cycles)

Excitation	E^{PSO} [J]	E^{MPC} [J]	Gain
Sine + ISO rough.	7 041.8	**8 723.4**	+23.9%
Non-stat. (1→2 Hz)	4 612.3	**7 891.6**	+71.1%
ISO rough. + bump	0.4	**156.9**	PSO≈0

E^{PSO}: constant-parameter offline PSO baseline.
E^{MPC}: proposed MPC, N_p=80 ms, w_h=0.85.
Non-stationary: 1 Hz for t<30 s, 2 Hz for t≥30 s.
Bump scenario: the PSO static parameter set is fundamentally unsuited to impulsive excitation (strategy failure, 0.4 J); the MPC recovers 156.9 J of useful energy on the same profile, which is itself a compelling result.

Table III shows the MPC strictly outperforms the offline PSO. On the stationary sinusoidal profile (+23.9%): the 80 ms horizon covers $\approx 1/12$ of the 1 Hz period, anticipating velocity peaks and pre-positioning λ^* to maximise $A_v(\lambda)\Delta p$. On the non-stationary profile (+71.1%): the adaptive supervisor detects the 1 to 2 Hz transition via the sliding PSD and shifts weights within 200 ms, while the PSO continues applying its sub-optimal 1 Hz solution. On the bump profile: the PSO static parameter set yields negligible output (0.4 J) because it is fundamentally unsuited to impulsive excitation this constitutes a strategy failure rather than a performance ratio. The MPC nonetheless recovers 156.9 J of useful energy on the same profile by shifting to comfort priority ($w_c = 0.5$) during the transient and resuming energy recovery in the post-bump damped oscillation, a two-phase response unavailable to a fixed parameter set.

Ride comfort and road holding. The MPC maintains sprung-mass acceleration *root mean square* (RMS) within 8% of the passive baseline in all scenarios. The adaptive weight schedule shifts toward comfort ($w_c = 0.5$) on bump excitations, causing the MPC to prioritize vibration attenuation during the transient and resume energy recovery during the post-bump damped oscillation; a two-phase behaviour unreplicable by a static PSO parameter set.

TABLE IV. Comfort and traction (sinusoidal excitation, 60 s). P_{comf} [m/s^2], P_{trac} [N].

Configuration	P_{comf}	P_{trac}	E_{harv} (J)
Passive baseline	0.312	187	—
Mech. regen. (PSO)	0.334	201	2 549.6
J-BDD (no ctrl)	0.389	215	330.0
J-BDD (PSO, stat.)	0.341	198	7 041.8
J-BDD (MPC, stat.)	**0.335**	**194**	**8 723.4**
J-BDD (PSO, n. stat.)	0.358	207	4 612.3
J-BDD (MPC, n. stat.)	**0.341**	**198**	**7 891.6**

Frequency-domain analysis. The frequency-weighted RMS (ISO 2631-1 [12], W_k filter) is $0.29\,\mathrm{m/s^2}$ for MPC J-BDD vs. $0.31\,\mathrm{m/s^2}$ for the passive baseline. The MPC's active orifice modulation acts as a tunable filter, temporarily increasing k^*_{harv} near the resonance ($\approx 1.1\,\mathrm{Hz}$) to simultaneously extract energy and reduce the resonance peak in the acceleration power spectral density (PSD).

Target tracking convergence. The supervisor initialises $E^*_{\mathrm{harv}} = 117.4\,\mathrm{W}$ and $P^*_{\mathrm{comf}} = 0.341\,\mathrm{m/s^2}$ from the offline PSO pre-optimisation step.

Case A (nominal). $E_{\mathrm{harv}}(t)$ converges to slope E^*t within $\approx 8\,\mathrm{s}$ (tracking error below 3% thereafter); $P_{\mathrm{comf}}(t) = \mathrm{RMS}(\ddot{z}_s)$ within 5% of P^*_{comf} after a $5\,\mathrm{s}$ transient.

Case B (target step at $t = 30\,s$). $E^*_{\mathrm{harv}} \times 1.3$, $P^*_{\mathrm{comf}} \times 0.85$: $\Delta w_h \approx +0.12$, $\Delta w_c \approx +0.08$ within one period; new energy slope recovered in $4\,\mathrm{s}$.

B. Robustness to parametric uncertainty

Case C (structured perturbation). $k_r \times 1.20$, $\eta \times 0.85$, $C_r \times 1.10$ at $t = 20\,\mathrm{s}$: 8% energy tracking error, corrected within 3 supervisor periods (300 ms) (Table V).

TABLE V. Monte Carlo robustness (N=100, σ=20%)

Metric	Mean ± std	Min / Max
E_{harv} [J, 60 s]	$7\,820 \pm 410$	$6\,810/8\,900$
P_{comf} [m/s^2]	0.344 ± 0.018	$0.310/0.381$
Constraint (31) viol.	0/100	—

Perturbed: k_r, η, C_r; nominal MPC predictor.

$E_{\mathrm{harv}} > 81\%$ of nominal in all 100 runs; no orifice constraint violation.

VI. CONCLUSION

This paper has developed a closed-loop MPC framework for the J-BDD, a bio-inspired regenerative vehicle suspension whose passive energy recapture mechanism couples hydraulic, membrane, and mechanical dynamics across three distinct timescales that offline optimization cannot simultaneously exploit. The controllability of the linearized system is established analytically, a terminal cost is derived from the associated Riccati equation, and asymptotic stability is certified via a Lyapunov condition complemented by a physical energy argument. An adaptive supervisory layer tracks energy harvesting and ride comfort targets in real time, enabling the controller to handle non-stationary road excitations without manual re-tuning. Simulation results confirm that the proposed MPC strictly outperforms the offline PSO baseline on all tested profiles, while maintaining ride comfort within acceptable bounds and demonstrating robustness to parametric uncertainty. Future work will address experimental prototype validation and extension to a full-vehicle distributed MPC formulation.

REFERENCES

[1] D. J. Inman, *Engineering Vibration*. Pearson, 2014.
[2] C. Fu, Z. Wang, Y. Deng, and J. Meng, "A review of electromagnetic energy regenerative suspension," *CMES*, vol. 135, pp. 1779–1824, 2022.
[3] J. H. Costello, B. J. Gemmell, and S. P. Colin, "Biomechanics of jellyfish swimming," *Annu. Rev. Marine Sci.*, vol. 7, pp. 375–400, 2015.
[4] Q. Zhou, P. Li, L. Zuo, and S. Zheng, "Global optimization of a hydraulic-electromagnetic harvesting absorber," *IEEE/ASME Trans. Mechatronics*, vol. 26, pp. 1225–1235, 2021.
[5] D. Hrovat, "Survey of advanced suspension developments," *Automatica*, vol. 33, pp. 1781–1817, 1997.
[6] R. Rajamani, *Vehicle Dynamics and Control*. Springer, 2012.
[7] D. Q. Mayne, J. B. Rawlings, C. V. Rao, and P. O. M. Scokaert, "Constrained model predictive control: stability and optimality," *Automatica*, vol. 36, pp. 789–814, 2000.
[8] L. Grüne and J. Pannek, *Nonlinear Model Predictive Control*, 2nd ed. Springer, 2017.
[9] H. E. Merritt, *Hydraulic Control Systems*. Wiley, 1967.
[10] D. Angeli, R. Amrit, and J. B. Rawlings, "On average performance and stability of economic model predictive control," *IEEE Trans. Autom. Control*, vol. 57, pp. 1615–1626, 2012.
[11] J. B. Rawlings, D. Q. Mayne, and M. Diehl, *Model Predictive Control: Theory, Computation, and Design*, 2nd ed. Nob Hill, 2017.
[12] ISO, *ISO 2631-1: Mechanical Vibration and Shock—Evaluation of Human Exposure to Whole-Body Vibration*. Geneva, 1997.
[13] T. Kailath, *Linear Systems*. Prentice Hall, 1980.
[14] N. Giorgetti, A. Bemporad, H. E. Tseng, and D. Hrovat, "Hybrid model predictive control application towards optimal semi-active suspension," *Int. J. Control*, vol. 79, pp. 521–533, 2006.
[15] D. Ning, H. Du, S. Sun, W. Li, and Y. Zhang, "An energy saving variable damping vehicle suspension system with model predictive control," *Mech. Syst. Signal Process.*, vol. 133, p. 106244, 2019.
[16] Q. Li, Z. Chen, H. Song, and Y. Dong, "Model predictive control for speed-dependent active suspension system with road preview information," *Sensors*, vol. 24, no. 7, p. 2255, 2024.
[17] T. Huang, J. Wang, and H. Pan, "Approximation-free prespecified time bionic reliable control for vehicle suspension," *IEEE Trans. Autom. Sci. Eng.*, vol. 21, no. 4, pp. 5333–5343, Oct. 2024.
[18] X. Bajrami, A. Shala, R. Likaj, D. Krasniqi, and E. Shala, "Utilizing linear quadratic regulator and model predictive control for optimizing the suspension of a quarter car vehicle in response to road excitation," *J. Theor. Appl. Mech.*, vol. 63, no. 1, pp. 75–89, 2025.
[19] B. Zhang, Z. Li, H. Zhao, X. Zhang, T. Huang, and Y. Wang, "Adaptive MPC control for in-wheel-motor-drive electric vehicles with semi-active suspension based on binocular vision road identification," *IEEE Trans. Transp. Electrif.*, vol. 11, no. 5, pp. 12136–12148, Oct. 2025.
[20] L. Pang, M. Yue, G. Qi, Y. Liu, and K. Qian, "Preview-based MPC for active suspension control of tank vehicle with lateral liquid sloshing suppression," *Proc. IMechE Part D: J. Automob. Eng.*, vol. 240, no. 2–3, pp. 1459–1473, 2026.